VOL. 4, NO. 7, SEPTEMBER 2009 ISSN 1819-6608
ARPN Journal of Engineering and Applied Sciences


www.arpnjournals.com

FINITE ELEMENT MODELING AND SIMULATION OF CONTACT INTERACTION AND DEFORMATION OF CARBON FIBROUS COMPOSITE BEAM AGAINST RIGID INDENTER

Umar Farooq and Karl Gregory
Built Environment and Engineering Department, University of Bolton United Kingdom
E-Mail: uf1res@bolton.ac.uk, k.r.gregory@bolton.ac.uk

ABSTRACT

This study is concerned with finite element modeling and simulation of fibrous composite beams contact with rigid indenter. Mathematical formulations consisting of contact law and indentation wrapping have been developed. Fibrous orientated moduli and types quasi-isotropic materials were also presented. Finite element method software ABAQUS was chosen to perform simulation incorporating dynamic contact in time-domain using implicit dynamics routine. To improve convergence, mapped meshing techniques were employed to mesh the regions of high stress gradient with fine meshes and coarse meshes for the rest. Results from homogeneous beam were compared with the results from quasi-isotropic beams with 8, 12, and 24 plies and found to be in good agreement. The present study has demonstrated computationally model the contribution of fibre orientation effects on resulting damage and response of composite beams while interacting with rigid indenter.

Keywords: model, fibrous composite beams, finite element method, low-velocity impact, contact law, implicit dynamic.

1. INTRODUCTION

The superior properties of composite materials such as high strength to weight ratio, high creep resistance, high tensile strength at elevated temperature, and high toughness have garnered higher interest in numerous automotive, aerospace, and sports applications.

Many of aircraft components are manufactured in such a way that the parts can be disassembled for shipping, inspection, repair, and/or replacement. Normally beams are used as load carrying and supporting or different fasteners to join the different components. Composite beams are being used in civil, transport and aerospace structures instead of metal beams and bars.

However, foreign object contacts on the beams often dictate the design allowable of the entire structure. The mechanical properties of structures subjected to such contacts are dependent upon the damage size, laminate size and thickness, and ply size, thickness and orientation. All of these factors affect damage initiation, ply interaction within the structure and extent of damage growth and require good understanding of composites' responses for improved and safe design which could avoid catastrophic failures.

To predict the contact behaviour and the overall deformation of the target, a detailed model of the contact region is necessary. A simple relationship between the contact force and the indentation was used to study the impact of a beam by a steel sphere by Timoshenk [1-2]. This approach has been used extensively since then and is commonly used for the analysis of impact on composite materials. Results in this field have since been extended to all branches of engineering, but are most essential in the study of tribology and indentation hardness.

A series of paper on this subject has been published from late 1970s to 1980s [4, 5, 6, 7 and 8]. Since 1980s many researchers have tried to analytically investigate low-velocity impact response and damage of composite structures. Some review papers on the subject have been published [2-3].

After the publication of this series of paper by C.T. Sun and his pupils, many researchers have studied the low-velocity impact problem on composite laminates following his approach [9-11]. The modified Hertzian contact law proposed and applied in the low-velocity impact response of composite laminates [4]. Experimental indentation law through static indentation tests on composite laminates are given in [5-6]. Finite element program to analyze impact response of composite laminates using pendulum type low-velocity impact test system [6-8]. New approach for simple prediction of impact force history on composite laminates was proposed in [14-15].

In the present study, parametric study on contact law superposition of deformed region was performed through changing the number of plies and fibre orientations. The approach shows that conventional beams could be conveniently replaced by the composite beams where out-of-plane contact is expected. Moreover, the models could be applied to areas where contact analysis problem using finite element software in design analysis and developments.

2. THE MATHEMATICAL FORMULATIONS

2.1 The contact between two elastic solids

Contact mechanics is the study of the deformation of solids that touch each other at one or more points. Complex forces and moments are transmitted between the bodies where they touch. The contacted area of physics restricted in which the motion of two or more bodies in space is restricted by additional constraints. These so called unilateral constraints ensure that bodies

once coming into contact do not penetrate each other. Once the general equations for a contact problem are set up, different solution schemes can be used to simulate the behaviour of bodies in contact and to compute displacement and stress fields. There are several possibilities to classify contact problems. Generally contact with and without friction is distinguished.

Contact may occur between bodies in two distinct ways. A conforming contact is one in which the two bodies touch at multiple points before any deformation takes place (i.e., they just "fit together"). The opposite is non-conforming contact, in which the shapes of the bodies are dissimilar enough that, under no load, they only touch at a point (or possibly along a line). In the non-conforming case, the contact area is small compared to the sizes of the objects and the stresses are highly concentrated in this area.

Assumptions of hertz

- Contacting bodies are locally spherical;
- Contact radius << dimensions of the body;
- Linear elastic and isotropic material properties;
- Neglect friction;
- Neglect adhesion;
- Hertz developed this theory as a graduate student during his 1881 Christmas vacation; and
- What will you do during your Christmas vacation.

A frame of reference is defined in which the objects (possibly in motion relative to one another) are static interact through surface tractions (or pressures/stresses) at their interface. The indentation, the difference between the displacement of the projectile and that of the back face of the laminate, can be of the same order as or longer than the overall displacement of the laminate.

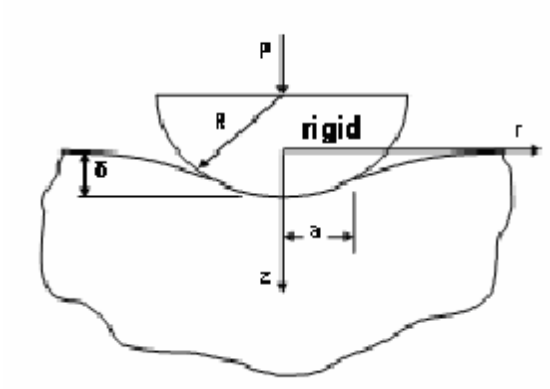

Figure-1. Two bodies of revolution for Hertzian the contact zone.

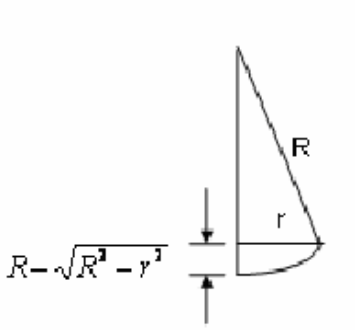

Figure-2. Radii of rigid indenter and target.

Defining the parameters R and E as

$$\frac{1}{R}=\frac{1}{R_1}+\frac{1}{R_2},\quad \frac{1}{E}=\frac{1-\nu_1^2}{E_1}+\frac{1-\nu_2^2}{E_2}, \tag{1}$$

Radii of curvatures of the two bodies are R_1 and R_2. The Young's moduli and Poisson's ratios of the two bodies are E_1, v_1, and E_2, v_2, respectively. Without loss of generality, the subscript 1 is taken to denote properties of the indenter and subscript 2 identifies properties of the target. The radius of the contact zone "a", the relative displacement "α", and the maximum pressure are given by

$$a=\left(3\frac{PR}{4E}\right)^{\frac{1}{3}}\ ;\ P_0=\frac{3P}{2\pi a^2}=\left(\frac{6PE^2}{\pi^3 R^2}\right)^{\frac{1}{3}}\ ;$$

$$\alpha=\frac{a^3}{R}=\left(\frac{9P^2}{16RE^2}\right)^{\frac{1}{3}} \tag{2}$$

The contact force, P, is usually related to the indentation by the Hertz contact law, derived assuming contact between two smooth elastic, homogenous, isotropic solid bodies of revolution Eq (1). For two isotropic bodies of revolution (Figure-1), contact occurs in a circular zone of radius a in which the normal pressure p varies as

$$p=p_0\left[1-\left(\frac{r}{a}\right)^2\right]^{\frac{1}{2}} \tag{3}$$

Where P_0 is the maximum contact pressure at the centre of the contact zone and r is the radial position of an arbitrary point in the contact zone. The force indentation law is expressed as

$$P=k\alpha^{\frac{3}{2}} \tag{4}$$

Where P is the contact force, α is the indentation, and the contact stiffness k is given by

$$k=\frac{4}{3}R^{\frac{1}{2}} \tag{5}$$

Equation (4) is usually referred to as *Hertz contact law or the Hertizian law of contact* and is found to apply for a wide range of cases, even if all assumptions made in the derivation of the theory are not satisfied. Same pressure on a small circular region of a locally spherical body will produce same change in curvature given by:

$$p(r) = p_0\sqrt{1-(r/a)^2}, \quad r < a \tag{6}$$

Gives a spherical depression and hence is the pressure for Hertz contact, i.e. for the indentation of a flat elastic body by a rigid sphere with deflection and radius of curvatures Eq. (2) change to

$$\delta = \frac{(1-\nu^2)\pi}{2E} p_0 a$$
$$\frac{1}{R} = \frac{(1-\nu^2)\pi\ p_0}{2Ea} \tag{7}$$

2.2 Indentation and wrapping with contact zones

During the indentation of beams, local deformations are superposed onto the overall deflection of the beam. When the beam deflections are small, the interaction between the local indentation and the overall deflection of the beam is negligible. Therefore, the indentation law and the pressure distribution in the contact zone are the same as for the indentation of a half-space. However, for flexible beams under large indenters, the beam theory may wrap around the indenter, leading to significant changes in the normal pressure distribution.

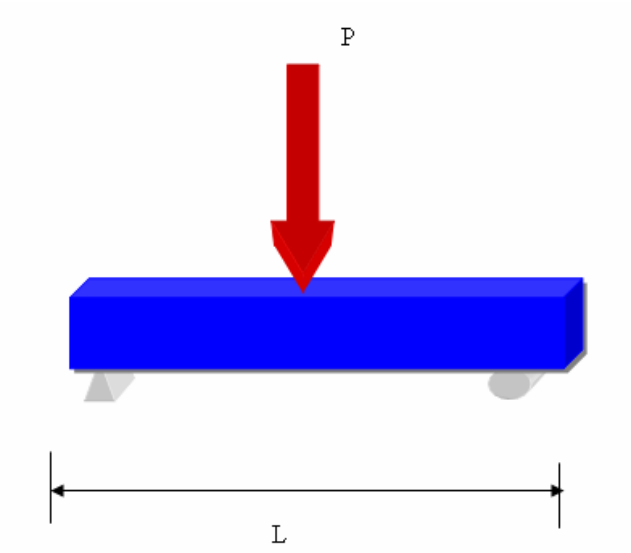

Figure-3. Simply supported beam with concentrated force applied in centre.

From the beam theory the axial displacements are related to the transverse displacements by

$$w(x,z) = -z\frac{dw(x)}{dx}$$ And the axial strain is

$$\varepsilon_{xx} = -z\frac{d^2w(x)}{dx^2}$$

Bending moment is related to the transverse displacement by

$$M = -\int_A \sigma_{xx} z dA = -\int_A E\varepsilon_{xx} z^2 dA$$
$$= \int_A E\varepsilon_{xx} z^2 dA \frac{d^2w}{dx^2} = EI\frac{d^2w}{dx^2} \tag{8}$$

The bending moment distribution in a simply supported beam of length L subjected to a concentrated force applied in the centre (Figure-3) is given by

$$M = \frac{P}{2}\left(\frac{L}{2} - x\right) \tag{9}$$

For x > 0.The curvature of the beam is given by the second derivative of the deflection. Using Eq. (10) and Eq. (11), the load required to bend the beam to a radius R equal to that of the indenter is found to be

$$P = \frac{4EI}{RL} \tag{10}$$

Which indicates that wrapping is more likely to occur for long flexible beams under a large impactor.

As the load increase, the beam comes in contact with the indenter over a distance a (Figure-4). In that region, the radius of curvature is constant and equal to the radius of the impactor. Equation (8) implies that the bending moment is also constant, and the shear force is uniformly equal to zero and the pressure under the impactor is zero. The beam is then loaded by two concentrated forces of magnitude "P/2" loaded at "+a and –a". The distance a is such that the curvature of the beam at x = a is equal to the

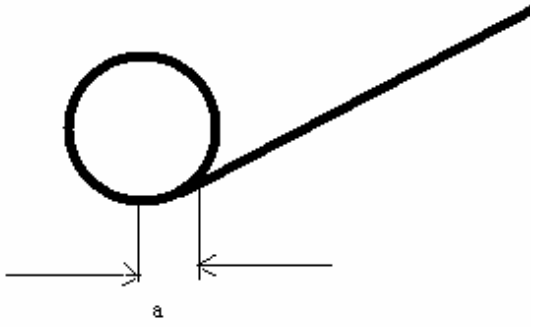

Figure-4. Beam wrapping around the indenter.

Curvature of the indenter. For a < x < L/2, the bending moment is given by Eq.(9), and using Eq.(8) we find

$$A=\frac{L}{2}-\frac{2EI}{PR} \tag{11}$$

For value of "P" larger than that given by Eq. (10). The conclusion from this simple analysis is that, neglected local deformations, as a concentrated contact force would produce radius of curvature smaller than the radius of the indenter, the beam is loaded by two forces separated by a distance "2a". When local deformations are included, the pressure distribution is expected to be such that the maximum pressure is reached close to the edge of the contact zone. The non-dimensional contact pressure is given by

$$\overline{P}=\left(1-x^2\right)^{\frac{1}{2}}\left[1-\beta\left(1-4\overline{x}^2\right)\right] \tag{12}$$

Where $\overline{x}=x/c$, with c being the radius of the contact zone. The non-dimensional contact pressure is related to the actual pressure by

$$\overline{P}=\frac{\pi bc}{2P}\,p(x) \tag{13}$$

$$\overline{c}=c/l,\ \beta=8.75\,B\,\overline{c}^{4},$$

$$B=\frac{\pi}{32}\frac{D_2}{D_1}\left(l/h\right)^3$$

$$and\quad D_1=\frac{E_1}{\left(1-\nu_{12}^2\right)};$$

$$D_2=\frac{2E_2}{\left(\lambda_1+\lambda_2\right)}.\ \lambda_1\ and\quad \lambda_2$$

With are the roots of the bi-quadratic equation

$$S_{11}\lambda^4-\left(2S_{12}+S_{66}\right)\lambda^2+S_{22}=0. \tag{14}$$

Where the components of the compliance matrix of the material are defined as
$S_{11} = 1/E_1$, $S_{22} = 1/E_2$, $S_{12} = - \nu_{12}/E_1$,
$S_{66} = 1/G_{12}$.

For small values of β, the actual pressure follows a Hertzian distribution Eq. (4), but as β increases, the pressure is distributed more towards the edge of the contact zone as predicted by the beam analysis. For the case of a flat target indented by a hemispherical indenter, R_2 reduces to zero and equation becomes:

$$n=\frac{4E\sqrt{R_1}}{3} \tag{15}$$

2.3 Material characterization equations

2.3.1 Static Equilibrium Equations (Conservation of Linear Momentum)
For a linear elastic solid under static equilibrium, the following equations for any 3-D body can be written:

$$\begin{aligned}
&\frac{\partial \sigma_{xx}}{\partial x}+\frac{\partial \sigma_{yx}}{\partial y}+\frac{\partial \sigma_{zx}}{\partial z}+\rho g_x=0\\
&\frac{\partial \sigma_{xy}}{\partial x}+\frac{\partial \sigma_{yy}}{\partial y}+\frac{\partial \sigma_{zy}}{\partial z}+\rho g_y=0\\
&\frac{\partial \sigma_{xz}}{\partial x}+\frac{\partial \sigma_{yz}}{\partial y}+\frac{\partial \sigma_{zz}}{\partial z}+\rho g_z=0
\end{aligned} \tag{16}$$

2.3.2 Constitutive equations (Material response to stress or strain)

$$\sigma_{xx} = \frac{E}{(1+\nu)(1-2\nu)}[(1-\nu)\varepsilon_{xx} + \nu\varepsilon_{yy} + \nu\varepsilon_{zz}]$$
$$\sigma_{yy} = \frac{E}{(1+\nu)(1-2\nu)}[\nu\varepsilon_{xx} + (1-\nu)\varepsilon_{yy} + \nu\varepsilon_{zz}]$$
$$\sigma_{zz} = \frac{E}{(1+\nu)(1-2\nu)}[\nu\varepsilon_{xx} + \nu\varepsilon_{yy} + (1-\nu)\varepsilon_{zz}]$$
$$\sigma_{xy} = \frac{E}{(1+\nu)}\varepsilon_{xy} \qquad (17)$$
$$\sigma_{xz} = \frac{E}{(1+\nu)}\varepsilon_{xz}$$
$$\sigma_{yz} = \frac{E}{(1+\nu)}\varepsilon_{yz}$$

2.3.3 Geometric relations (Kinematics) for small strain

$$[\varepsilon] = \begin{bmatrix} \varepsilon_{xx} & \varepsilon_{xy} & \varepsilon_{xz} \\ \varepsilon_{yx} & \varepsilon_{yy} & \varepsilon_{yz} \\ \varepsilon_{zx} & \varepsilon_{zy} & \varepsilon_{zz} \end{bmatrix}$$
$$= \begin{bmatrix} \frac{\partial u_x}{\partial x} & \frac{1}{2}(\frac{\partial u_y}{\partial x} + \frac{\partial u_x}{\partial y}) & \frac{1}{2}(\frac{\partial u_z}{\partial x} + \frac{\partial u_x}{\partial z}) \\ \frac{1}{2}(\frac{\partial u_x}{\partial y} + \frac{\partial u_y}{\partial x}) & \frac{\partial u_y}{\partial y} & \frac{1}{2}(\frac{\partial u_z}{\partial y} + \frac{\partial u_y}{\partial z}) \\ \frac{1}{2}(\frac{\partial u_x}{\partial z} + \frac{\partial u_z}{\partial x}) & \frac{1}{2}(\frac{\partial u_y}{\partial z} + \frac{\partial u_z}{\partial y}) & \frac{\partial u_z}{\partial z} \end{bmatrix} \qquad (18)$$

2.4 Relations between orientation of fibres and elastic moduli

A composite material is heterogeneous with properties changing from point to point. The anisotropic properties associated with an axis passing through a point depend on the orientation of the axis. The generalized stresses to strain can be written as,

$$\sigma_i = C_{ij}\varepsilon_j \qquad \text{i, j = 1, ..., 9} \qquad (19)$$

Where 'C' is a fully populated 9 x 9 matrix of 81 elastic constants. Since both stresses and strains are symmetric so that there only six independent strain components and the

number of nonzero elastic constants reduce to 36 in the Eq (10).

$$[C]=\begin{bmatrix} C_{11} & C_{12} & C_{13} & C_{14} & C_{15} & C_{16} \\ C_{12} & C_{22} & C_{23} & C_{24} & C_{25} & C_{26} \\ C_{13} & C_{23} & C_{33} & C_{34} & C_{35} & C_{36} \\ C_{14} & C_{24} & C_{34} & C_{44} & C_{45} & C_{46} \\ C_{15} & C_{25} & C_{35} & C_{45} & C_{55} & C_{56} \\ C_{16} & C_{26} & C_{36} & C_{46} & C_{56} & C_{66} \end{bmatrix} \quad (20)$$

Elastic materials for which an elastic potential or strain energy density function exists have incremental work per unit volume of, $dW = \sigma_i d\varepsilon_i$ resulting in 21 independent constants

$$[C]=\begin{bmatrix} C_{11} & C_{12} & C_{13} & C_{14} & C_{15} & C_{16} \\ 0 & C_{22} & C_{23} & C_{24} & C_{25} & C_{26} \\ 0 & 0 & C_{33} & C_{34} & C_{35} & C_{36} \\ 0 & 0 & 0 & C_{44} & C_{45} & C_{46} \\ 0 & 0 & 0 & 0 & C_{55} & C_{56} \\ 0 & 0 & 0 & 0 & 0 & C_{66} \end{bmatrix} \quad (21)$$

For an orthotropic material the stress-strain relation of a symmetric case can be represented by 9 independent constants and 12 nonzero terms. The resulting stiffness matrix for orthotropic material is:

$$[C]=\begin{bmatrix} C_{11} & C_{12} & C_{13} & 0 & 0 & 0 \\ C_{12} & C_{22} & C_{23} & 0 & 0 & 0 \\ C_{13} & C_{23} & C_{33} & 0 & 0 & 0 \\ 0 & 0 & 0 & C_{44} & 0 & 0 \\ 0 & 0 & 0 & 0 & C_{55} & 0 \\ 0 & 0 & 0 & 0 & 0 & C_{66} \end{bmatrix} \quad (22)$$

For plane stress in an orthotropic lamina,

$\sigma_3 = 0 \qquad \tau_{23} = 0 \qquad \tau_{13} = 0$

Therefore,

$\varepsilon_3 = 0 \qquad \gamma_{23} = 0 \qquad \gamma_{13} = 0$

In such cases the independent constants reduces to four. Thus, the stiffness matrix for orthotropic material subjected to plane stress can be written as:

$$[C]=\begin{bmatrix} C_{11} & C_{12} & 0 \\ C_{12} & C_{22} & 0 \\ 0 & 0 & C_{66} \end{bmatrix} \quad (23)$$

For an isotropic material, all planes are planes of material symmetry and are Isotropic. There are two independent elastic constants associated with isotropic material and 12 nonzero terms in the stiffness matrix. The resulting stiffness matrix for an isotropic material is:

$$[C]=\begin{bmatrix} C_{11} & C_{12} & C_{12} & 0 & 0 & 0 \\ C_{12} & C_{11} & C_{12} & 0 & 0 & 0 \\ C_{12} & C_{12} & C_{11} & 0 & 0 & 0 \\ 0 & 0 & 0 & C_{44} & 0 & 0 \\ 0 & 0 & 0 & 0 & C_{44} & 0 \\ 0 & 0 & 0 & 0 & 0 & C_{44} \end{bmatrix} \quad (24)$$

Where $C_{44} = \dfrac{C_{11} - C_{22}}{2}$

2.5 Quasi-isotropic materials

In quasi-isotropic materials the in-plane effective elastic response of laminates is isotropic and composite behaves like an isotropic plate. The in-plane behaviour of composites is similar to that of isotropic plate, but the bending behaviour of quasi-isotropic laminate is different from isotropic plates. All symmetric laminates with 2N equal thickness layers (N > = 3) angles between fibre orientations are quasi-isotropic. A laminate is quasi-isotropic when there are at least 4 fibre directions; the number of plies in each direction is the same: and each ply is made of the same material and has the same thickness.

For both quasi-isotropic and isotropic laminates, A_{22} and A_{66} are $A_{22} = A_{11}$ and $(A_{11}-A_{12})/2$. There is no shear extension coupling and the matrix [A] is independent of the coordinate directions. Elements A_{16} and A_{26} are zero and $A_{66} = (A_{11}-A_{12})/2$ for symmetrical and unsymmetrical quasi-isotropic laminates. Practical composite structures are built with laminates having several layers with various orientations. The layer orientations are chosen to provide adequate stiffness and strength in the direction of the applied loads, taking into account that the composite material is much stronger and stiffer in the fibre direction than in any other direction. In a quasi-isotropic laminate, each layer has an orientation given by

$$\theta_k = k\theta/N + \theta_0 \quad (25)$$

Where k indicates the layer number, N is the number of layers (at least 3), and θ_0 is an arbitrary initial angle. Examples of quasi-isotropic laminates are with angles θ_k between fibres of 60, 45, 36, 30, etc.

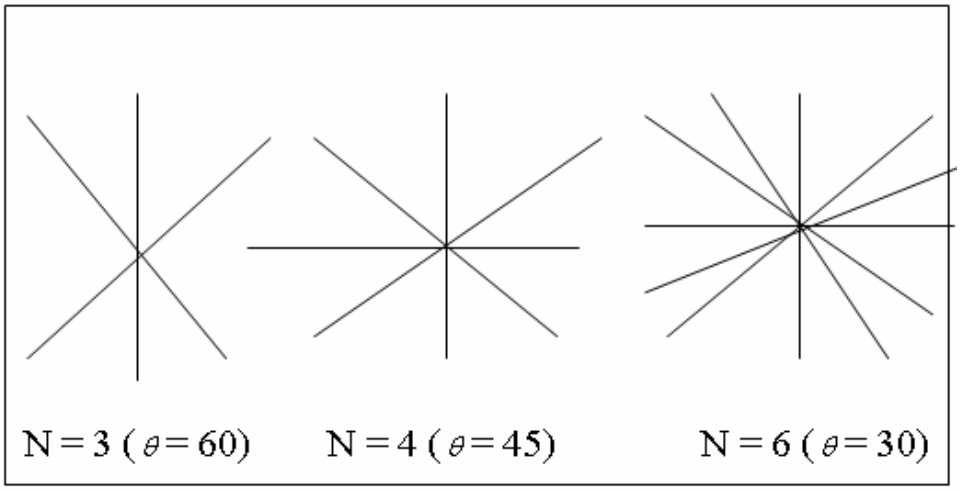

Figure-5. Ply orientations for quasi-isotropic lay-up.

When writing the stacking sequence, any angle less than 90 degree is replaced by its complement (for $\theta_k > 90 \Rightarrow \theta_k = \theta_k - 180$). For example, [60/120/180] is rewritten as [60/-60/0]. The layers can be ordered in any order, like [60/0/-60], and laminate is still quasi-isotropic. Quasi-isotropic laminates are in general not symmetric, but they can be made symmetric by doubling the number of layers in a mirror (symmetric) fashion. Since all layers are of equal thickness, take the layer thickness to be $t_k = 2H/2N = H/N$ with equal layer thickness t and total laminate thickness 2H = 4Nt.

2.6 Stress strain relations for composite beams

From classical laminate plate theory, the extensional stiffness matrix [*A*] relates the in-plane forces {*N*} to the mid-plane strains {ε^o} and the bending stiffness matrix [*D*] relates the moments {*M*} to the curvatures {κ}. The coupling stiffness matrix [*B*] couples the in-plane forces {*N*} with the curvatures {κ} and the moments {*M*} with the mid-plane strains {ε^o}. Where $(Q_{ij})_h$ is the reduced stiffness for layer *h*, which is a function of the layer angle, θ_h, and the layer in-plane orthotropic engineering constants, *E*'s and ν's. Z_h and Z_{h-1} are the *Z* co-ordinates of the top and bottom surfaces of the *h* layer respectively. Considering a laminate made of "N" layers (lamina) of thickness "t" arranged as shown below.

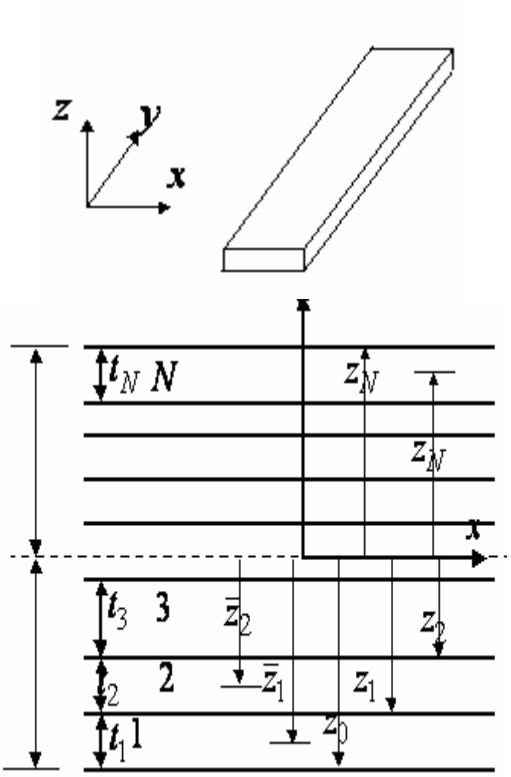

Error! No text of specified style in document.

Figure-6. Plies lay-up in a laminated beam.

Both the mid-surface strains {ε_{xo}, εyo, ε_{xy0}} and curvatures {K) are independent of z for the laminated plate, i.e., (z = 0) and the curvature of each lamina is the same and the Eqs can be written as:

$$\begin{Bmatrix}\sigma_1\\ \sigma_2\\ \sigma_6\end{Bmatrix}^k = \begin{bmatrix}Q_{11} & Q_{12} & 0\\ Q_{12} & Q_{22} & 0\\ 0 & 0 & Q_{66}\end{bmatrix}^k \begin{Bmatrix}\varepsilon_1\\ \varepsilon_2\\ \gamma_6\end{Bmatrix}^k$$

$$\begin{Bmatrix}\sigma_4\\ \sigma_5\end{Bmatrix}^k=\begin{bmatrix}Q_{44} & 0\\ 0 & Q_{55}\end{bmatrix}^k\begin{Bmatrix}\gamma_4\\ \gamma_5\end{Bmatrix}^k \quad (26)$$

The following laminate stiffness equations are obtained:

$$\begin{Bmatrix}N_x\\ N_y\\ N_{xy}\\ M_x\\ M_y\\ M_{xy}\end{Bmatrix}^k=\begin{bmatrix}A_{11} & A_{12} & A_{16} & B_{11} & B_{12} & B_{16}\\ A_{12} & A_{22} & A_{26} & B_{12} & B_{22} & B_{26}\\ A_{16} & A_{26} & A_{66} & B_{16} & B_{26} & B_{66}\\ B_{11} & B_{12} & B_{16} & D_{11} & D_{12} & D_{16}\\ B_{12} & B_{22} & B_{26} & D_{12} & D_{22} & D_{26}\\ B_{16} & B_{26} & B_{66} & D_{16} & D_{26} & D_{66}\end{bmatrix}^k\begin{Bmatrix}\varepsilon_x^0\\ \varepsilon_y^0\\ \gamma_{xy}^0\\ k_x\\ k_y\\ k_{xy}\end{Bmatrix}^k$$

$$\begin{Bmatrix}V_{yz}\\ V_{xz}\end{Bmatrix}^k=\begin{bmatrix}H_{44} & H_{45}\\ H_{45} & H_{55}\end{bmatrix}^k\begin{Bmatrix}\gamma_{yz}\\ \gamma_{xz}\end{Bmatrix}^k \quad (27)$$

Where the A, B and D coefficients are given by

$$A_{ij}=\sum_{k=1}^{N}\left(\overline{Q}_{ij}\right)_k\left(z_k-z_{k-1}\right)=\sum_{k=1}^{N}\left(\overline{Q}_{ij}\right)_k t_k$$

$$i,j=1,2,6$$

$$B_{ij}=\frac{1}{2}\sum_{k=1}^{N}\left(\overline{Q}_{ij}\right)_k\left(z^2{}_k-z^2{}_{k-1}\right)=\sum_{k=1}^{N}\left(\overline{Q}_{ij}\right)_k t_k z_k$$

$$i,j=1,2,6$$

$$D_{ij}=\frac{1}{3}\sum_{k=1}^{N}\left(\overline{Q}_{ij}\right)_k\left(z^3{}_k-z^3{}_{k-1}\right)=\sum_{k=1}^{N}\left(\overline{Q}_{ij}\right)_k\left(t_k z_k^2+\frac{t_k^3}{12}\right)_k$$

$$i,j=1,2,6$$

with

$$\begin{Bmatrix}V_x\\ V_y\end{Bmatrix}=\begin{bmatrix}H_{44} & H_{45}\\ H_{45} & H_{55}\end{bmatrix}\begin{Bmatrix}\gamma_{yx}\\ \gamma_{xz}\end{Bmatrix}$$

$$H_{ij}=\frac{5}{4}\sum_{k=1}^{N}\overline{Q}_{ij}\left[t_k-\frac{4}{t^2}\left(t_k\overline{z}_k^2+\frac{t_k^3}{12}\right)\right]$$

$$i,j=4,5 \quad (28)$$

The 6 x 6 stiffness matrix in Eq. (27) is composed of three sub-matrices, [A], [B], [D], [H] these coefficients are functions of thickness, orientation, stacking sequence, and material properties of the layers. Each matrix has particular role in the analysis.

3. NUMERICAL MODELING AND LOADING

Four independent models were developed in ABAQUS the first model consists of homogeneous material properties while the rest of the three were of quasi-isotropic material properties. All models were fully clamped in y-direction, free in x-direction and load was applied in the z-direction. The schematic diagram of the model is given in Figure-7; the other specifications are given as:

a) A homogeneous beam of Young's modulus 150 Gpa and Posson's ratios of 0.3 with 300 mm x 20 x 2.88 mm dimensions;
b) A quasi- isotropic beam of uni-directional material with Young's modulus 150 GPa, shear moduli of 15 GPa, and Posson's ratios of 0.3 of 300 mm x 20 x 2.88 mm (consisting of 8-ply with each ply 0.00036 mm thick);
c) A quasi- isotropic beam of uni-directional material with Young's modulus 150 GPa, shear modulii of 15 GPa, and Posson's ratios of 0.3 of 300 mm x 20 x 2.88 mm (consisting of 16-ply with each ply 0.00018 mm thick); and
d) A quasi- isotropic beam of uni-directional material with Young's modulus 150 GPa, shear modulii of 15 GPa, and Posson's ratios of 0.3 of 300 mm x 20 x 2.88 mm (consisting of 24-ply with each ply 0.00012 mm thick).

A steel indenter of 15 mm x 15 mm x 15 mm dimensions of Young's modulus 209 GPa and Poisson's ratios 0.3 were considered. It was assumed that any cross-section of beam remains plane after load. Friction in areas of contact was not considered.

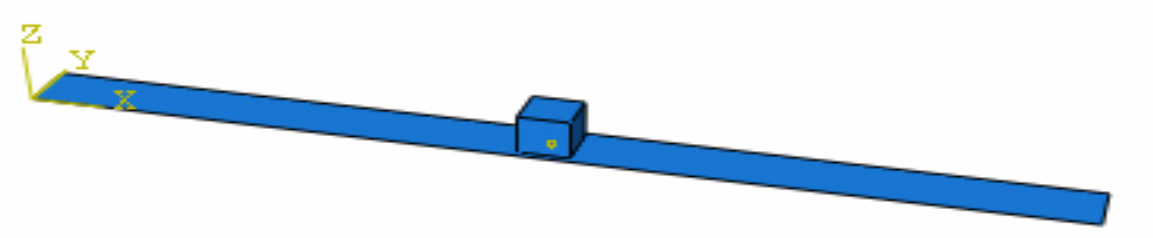

Figure-7. Plies lay-up in a beam with transverse contact from the indenter.

A downward load of 200 N is applied at the centre of the beam. The load was applied in increments of 10 N restricting to small-contact stage not getting into the region where indentation starts decreasing as the contact force is increased. All the models were run for one second with ten-thousand iterations in implicit dynamic time steps.

4. NUMERICAL RESULTS AND DISCUSSIONS

Strains were selected from the bulk of the results of four models. A fine mesh was used near the expected contact region in order to predict the contact displacements and strains pressure and contact area accurately.

4.1 Effect of fibre orientation on contact areas

To study the effect of contact areas, three types of laminate thickness models 8-ply (ply thickness = 0.00036 mm); 16-ply (ply-thickness = 0.00018 mm) and 24-ply (ply thickness = 0.00012) were studied. Since thickness for all the models was kept constants the internal variation of the fibrous direction did not have much effect on the surface areas as depicted in the plot given below.

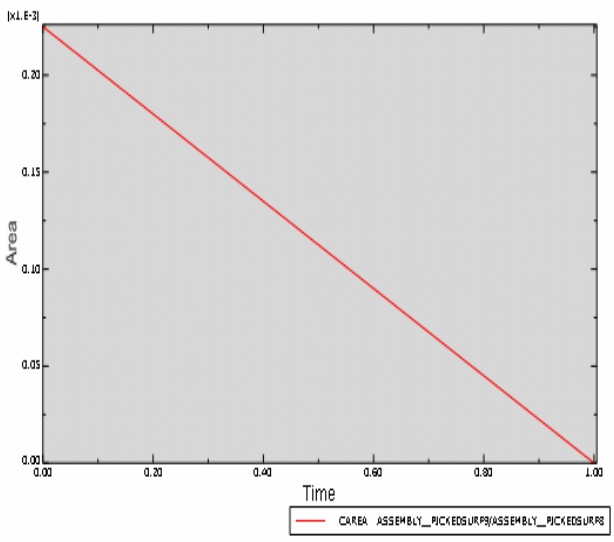

Figure-8.Graph of contact area of homogeneous beam model with similar graphs for the other mod.

4.2 Effect of fibre orientations on stresses

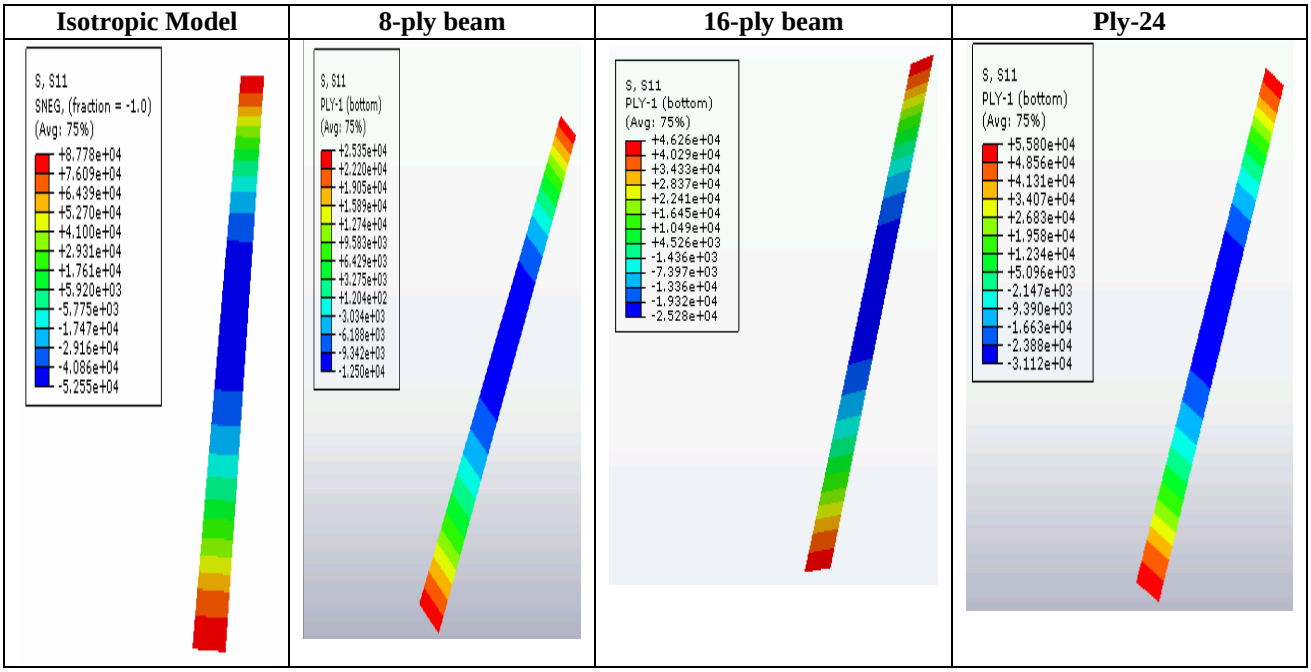

Figure-9. Legend table and contour plot of stresses produced in ply1 of fibrous beam models.

4.3 Effect of fibre orientation on strains

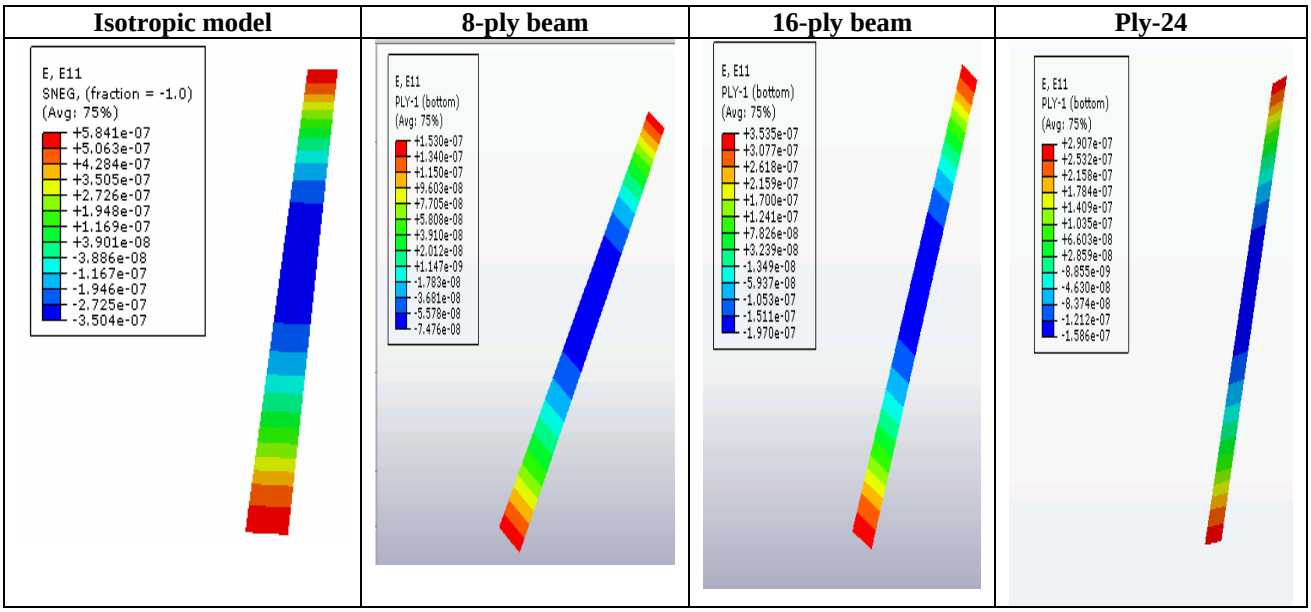

Figure-10. Legend table and contour plot of strains produced in ply 1 of fibrous model.

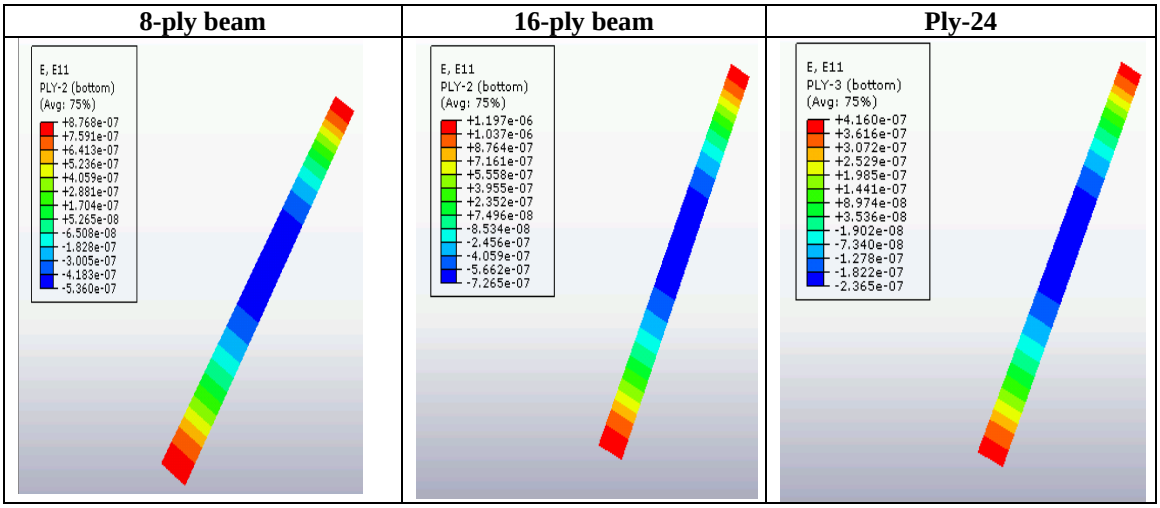

Figure-11. Legend table and contour plot of strains produced in ply 2 of fibrous model.

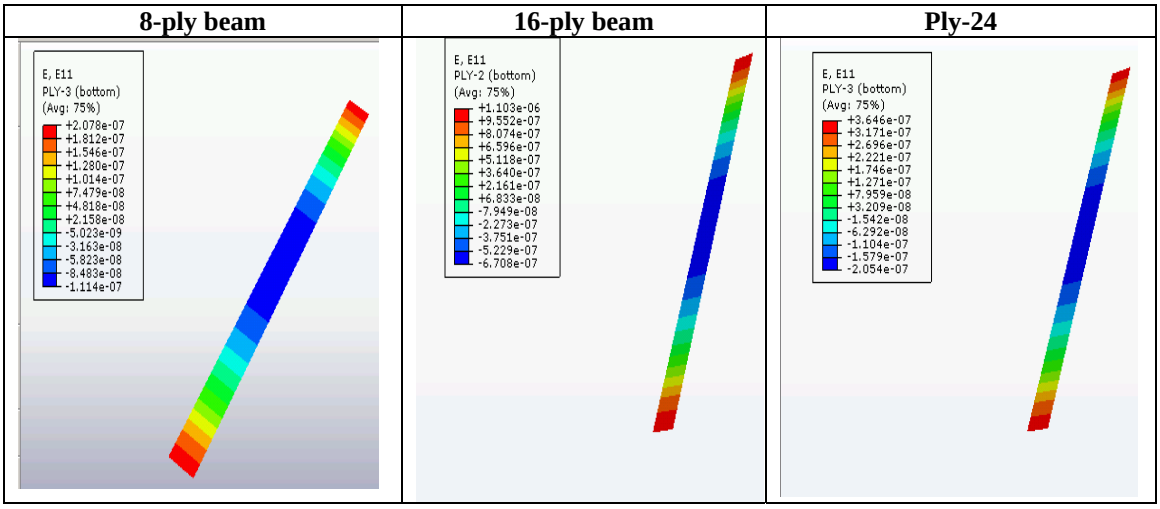

Figure-12. Legend table and contour plot of strains produced in ply 3 of fibrous model.

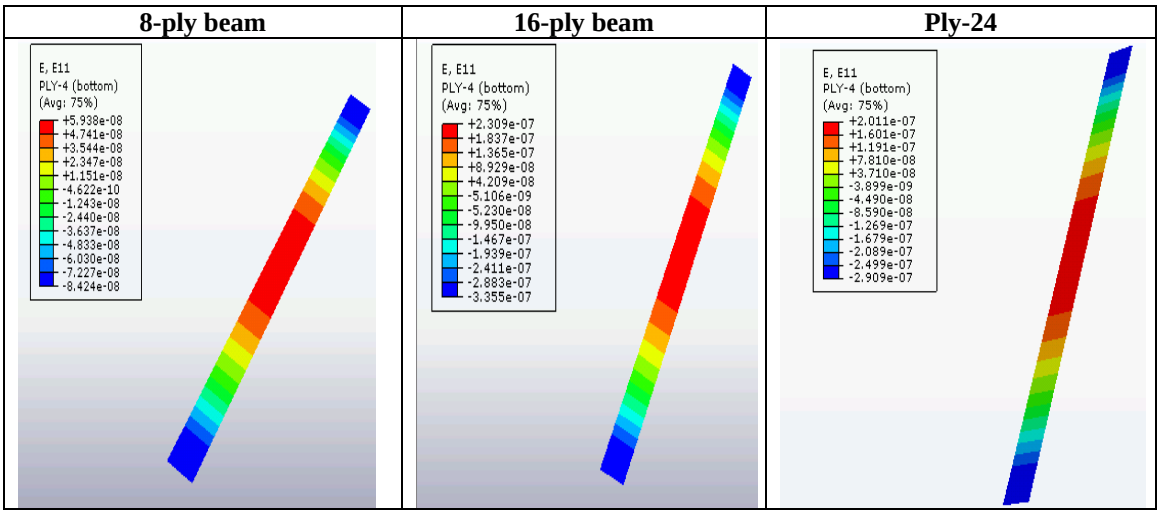

Figure-13. Legend table and contour plot of strains produced in ply 4 of fibrous model.

The effect of fibre orientations in stacking sequence on produced strains by contact have been shown in Figs.11-15 above. Fibre orientations in models have shown significant variation in the strains as well. On comparison, for orientation angles, the strains in 0^0 ply was larger than for the other cases. For the [45/0/-45/90] s plies the maximum strains are lower than the homogeneous beam. In general, the lower the flexural modulus, the easier it is for the beam to conform to the indenter shape and therefore, lower is the peak strains.

5. CONCLUSIONS

In this paper, contact effect of fibre orientations in fibrous composite beams was studied. With composite materials, permanent deformations were observed in the contact zone for relatively low force levels, but the material was assumed to remain linear elastic in the analysis. Differences in strain results were observed due to fibre orientations. Despite the fact that laminated composite materials are not homogenous or isotropic it describes fairly well the contact behaviour for carbon epoxy beams using modified Hertzian contact laws. Next, parametric study on contact law was performed through changing orientation of fibres in models. It was observed if the target was sufficiently flexible to give large global deflections "w", then 'wrapping' of the target around the indenter may occur. This may increase the contact area significantly, leading to a modified contact force distribution.

Finally, the result could also be applied to some of the similar low-velocity impact response analysis problems.

REFERENCES

[1] Shtaerman I. J. 1949. Contact Problem of Theory of Elasticity. Moscow.

[2] Timoshenko S. P. and J. M. Goodier. 1951. Theory of elasticity. McGrow Hill, New York.

[3] J.R. Willis. 1966. Hertzian contact of anisotropic bodies. J. Mech. Phys. Solids. 14: 163-176.

[4] Muskhelishvily N. I. 1996. Some Basic Problems of the Mathematical theory of Elasticity. Moskow. p. 708.

[5] Yang SH, Sun CT. 1981. Indentation law for composite laminates. Am. Soc. Test. Mater. ASTM STP. 787: 425-449.

[6] Teply M. I. 1983. The Contact Problems for areas with the Circular Boundaries. Lvov. p. 176.

[7] C.T. Sun and J.K. Chen. 1985. on the impact of initially stressed composite laminates. J. Compos. Mater. 19: 490-504.

[8] Tan T. M. and Sun C. T. 1985. Use of statistical indentation laws in impact analysis of comp. plates. J. Appl. Mech. 52: 6-12.

[9] Johnson K. 1987. Contact Mechanics. Cambridge University Press. p. 510.

[10] Sankar B. V. 1989. Smooth indentation of orthotropic beams. Compos. Sci. Technol. 34: 95-111.

[11] W.J. Cantwell and J. Morton. 1991. The impact resistance of composite materials a review. Composites. 22(5): 347-362.

[12] Robin Olsson and Soren Nilsson. 2006. Prediction of stresses in comp. plates under Hertzian law. J. Compos Constr. 73: 70-77.

[13] Tiberkak R, Bachene M. 2006. The dynamic response of comp. under low impact. 25th congress of Aero Sc., Hamburg, Germany.

[14] Wu E., Chao J. and Yen C. 1993. Smooth contact of orthotropic laminates by rigid cylinders. AIAA J. 31: 1916-1921.

[15] S. Abrate. 1994. Impact on laminated composite: recent advances. Appl. Mech. Rev. ASME. 47(11): 517-544.

[16] S. Abrate. 2001. Modeling of impacts on composite struct. Compos. Struct. 51: 129-138.

[17] 2004. ABAQUS/Standard Users' Manual. Version 6.7, Hibbitt, Karlsson and Sorenson, Inc., USA.